Treatment of mining wastewater polluted with cyanide by coagulation processes: a mechanistic study

Mamelkina Maria A., Herraiz-Carboné Miguel, Cotillas Salvador, Lacasa Engracia, Sáez Cristina, Tuunila Ritva, Sillanpää Mika, Häkkinen Antti, Rodrigo Manuel A.

DOI: 10.1016/j.seppur.2019.116345

Treatment of mining wastewater polluted with cyanide by coagulation processes: a mechanistic study

Maria A. Mamelkina[1], Miguel Herraiz-Carboné[2], Salvador Cotillas[2], Engracia Lacasa[2], Cristina Sáez[3], Ritva Tuunila[1], Mika Sillanpää[1], Antti Häkkinen[1], Manuel A. Rodrigo[3]*

[1] LUT School of Engineering Science, LUT University, P.O. Box 20 FI-53851 Lappeenranta, Finland

[2] Department of Chemical Engineering, School of Industrial Engineering, University of Castilla-La Mancha, 02071 Albacete, Spain

[3] Department of Chemical Engineering, Faculty of Chemical Sciences and Technologies, University of Castilla-La Mancha, 13005 Ciudad Real, Spain

Abstract

In this work, coagulation and electrocoagulation for the removal of cyanide ions contained in synthetic mining wastewater were evaluated paying particular attention to the elucidation of the coagulation mechanisms. Iron and aluminum salts with concentrations ranging from 0.01 to 10 000 mg dm^{-3} metal were used in chemical coagulation. Experimental data were properly fitted to Freundlich isotherm to elucidate that the main mechanism to remove cyanide during chemical coagulation was adsorption onto coagulant flocs although a maximum cyanide removal percentage of only 25% was attained. Then, electrochemical coagulation with iron and aluminum electrodes was evaluated at 1, 10 and 100 A m^{-2}, obtaining completely different results. Iron electrochemical coagulation leads to the complete cyanide removal regardless of the

current density applied, although the TOC removal was much lower than expected. On the contrary, only 60% of cyanide removal was reached by aluminum electrochemical coagulation and its efficiency was found to be highly dependent on the current density applied. Furthermore, no cyanate or hazardous inorganic chlorine species were detected during both electrocoagulation processes. However, chloride was oxidized to hypochlorite and then, it reacted with ammonium ions (contained in mining wastewater or produced by chemical reduction of nitrate by aluminum) to form chloramines. A proposal of coagulation mechanisms during the electrochemical process that explains experimental results was developed which involved the formation of iron-cyanide complexes, charge neutralization, adsorption on a superficially charged metal precipitate and/or enmeshment into a sweep metal floc.

Keywords: cyanide; mining wastewater; chemical coagulation; electrochemical coagulation; coagulation mechanisms

Highlights

- Cyanide is poorly removed by adsorption onto metal flocs in chemical coagulation.
- Iron electrochemical coagulation leads to a complete cyanide removal.
- Formation of soluble iron cyanide complexes allows reducing solution toxicity.
- Cyanide solubility decreases by charge neutralization with soluble $Al(OH)_3$.
- Null detection of cyanate or hazardous inorganic chlorine species.

*Corresponding author e-mail: manuel.rodrigo@uclm.es. Tel.: +34-926-29-53-00 Ext. 3411; fax: +34-926-29-52-56

1. Introduction

Free cyanide may be contained in industrial wastewater such as mining, metallurgical, petrochemical or coking wastewater [1-4]. About 13% of the 1.1 million metric tons of hydrogen cyanide produced annually worldwide is consumed by mining and metallurgical processes [5]. In mining processes, cyanide solutions are primarily used for the extraction of gold and silver from crushed ores. In addition, also they may be used to recover other metals such as copper, lead and zinc. The pH of cyanide solutions is a key parameter because free cyanide can be in the form of cyanide anion or volatile hydrocyanic acid, this last form being the predominant species for pH values below 8.5. Cyanide is considered a very toxic substance, because it can inhibit oxygen transfer to the cells due to its ability to bind iron in the blood by forming complexes and then, it can cause suffocation in animals and humans. The oral cyanide dose that is lethal to 50% of the exposed population ranges between 1 and 3 mg/kg of body weight.

The cyanide removal from industrial wastewater by conventional technologies has been widely reported during the last decade. Thus, cyanide may be degraded to ammonia by microorganisms under aerobic conditions [1] or it may be oxidized to less toxic cyanate by strong oxidizing agents such as hydrogen peroxide, hypochlorite and ozone [6]. In addition, it may be adsorbed on clays, feldspars and organic carbon, react with sulfur to form the seven-times less toxic thiocyanate and it may also strongly bind with various metals such as Fe, Cu, Ni, Mn, Pb, Zn, Cd, Sn or Ag to generate soluble and/or insoluble cyanide-metal complexes which are mostly non-reactive compounds [2, 3, 7-10].

Electrochemical technologies have recently emerged for industrial applications thanks to their simple equipment and easy automation in different environments and scales [11-16]. Furthermore, these technologies can be considered as environmentally friendly because

no addition of chemicals is needed and they can also be easily powered with green energy sources such as solar panels, windmills or fuel cells [17-20]. Among others, electrochemical oxidation, electro-Fenton and electrochemical coagulation have been reported to remove cyanide from industrial wastewaters. Both electrochemical oxidation and electro-Fenton leads to the oxidation of cyanide to cyanate and then, cyanate is mineralized to carbon dioxide and nitrogen. At this point, electrochemical oxidation attained around 90% of cyanide removal by using several anode materials such as mixed metal oxides, platinum, PbO_2 or boron doped diamond [21-23]. Likewise, electro-Fenton with reticulated vitreous carbon as cathode material reached over 90% of cyanide oxidation to cyanate by electrochemically generated hydrogen peroxide [24]. On the contrary, electrochemical coagulation is mainly based on the release of coagulants from a sacrificial anode. These species reduce the solubility of free cyanide in solution by different mechanisms. In literature, efficiencies over 90% for the removal of cyanides were reported by using electrochemical coagulation with iron electrodes, although no in-depth studies on removal mechanisms were found [25-27].

In this context, this paper mainly focuses on the development of coagulation mechanisms both in chemical and electrochemical coagulation processes to remove 100 mg dm^{-3} of cyanide in synthetic mining wastewater at alkaline pHs. To do this, standard jar test experiments were carried out by using iron and aluminum salts. Likewise, iron and aluminum electrodes inserted in a flow-by electrochemical reactor were tested under several current density values. Finally, the chemical reactivity of organic and inorganic species contained in solution was studied in order to rule out the formation of hazardous species.

2. Material and methods

2.1. Chemicals

Sodium cyanide and mining wastewater compounds [12] were of analytical grade and purchased from Panreac Química SLU. Chemicals to analyze cyanide were purchased from Merck and other chemicals used in several analyses were purchased from Sigma Aldrich, and each one was also analytical grade. Double deionized water of Millipore Milli-Q system with a resistivity of 18.2 MΩ cm at 25 ºC was used to prepare each solution.

2.2. Experimental procedures

Chemical coagulation experiments were developed by using the standard Jar-test technique. Each flask was filled with a volume of 500 mL of mining wastewater intensified with 100 mg CN^- dm^{-3}. Then the selected iron or aluminum chloride concentration was added, followed by the dosing of NaOH solution used for pH adjustment to a value of 12. After that, the mixture underwent 3 min rapid mixing and 12 min slow mixing. Then, after settling for 30 min, the supernatant liquid was filtered through a 0.20 µm filter and then, cyanide concentration was measured.

Electrochemical coagulation experiments were carried out in a single compartment flow cell working under batch operation mode [28, 29]. The electrodes placed in the electrochemical cell were made of iron and aluminum, and both anode and cathode materials were the same at each experiment. The electrode dimensions were 10 cm x 10 cm^2 and the net spacing between electrodes was 0.9 cm. The electric current was applied by using a Delta Electronika ES030-10 power supply characterized by the ranges 0-10 A and 0-30 V, and the current flowing through the cell was measured with a Keithley 2000

digital multimeter. Each experiment was carried out under galvanostatic conditions and the current densities applied were 1, 10 and 100 A m^{-2}. A volume of 2.0 L of mining wastewater intensified with 100 mg CN^- dm^{-3} (at initial pH of 12) were introduced into a glass tank and then, recirculated through the electrochemical cell using a peristaltic pump. Samples of 75 mL were collected each time and after settling time of 30 min, the supernatant liquid was filtered through a 0.20 μm filter for the determination of cyanide and other inorganic ions. TOC measurements were carried out without filtration. The chemical coagulation tests were performed during 15 minutes whereas electrochemical coagulation experiments were carried out during 540 minutes each one.

The chemical composition of the synthetic mining wastewater used has been previously reported elsewhere [12].

2.3. Analytical procedures

Cyanide concentrations were determined by silver nitrate titration method, which was initially introduced by Ryan and Culshaw [30]. The silver nitrate ($AgNO_3$) titration bases on the reactions produced by this salt in a cyanide media, where soluble silver cyanide complex ($Ag(CN)_2^-$) is firstly formed (Eq. 1), after which, the excess Ag^+ ions complex with rhodanine turning the color from a yellow to a pale pink. Further addition of $AgNO_3$ yields solid argentocyanide (AgCN) (Eq. 2). In this study, a modified standard method was used. $AgNO_3$ stock solution was further diluted to yield 0.00125 and 0.000125 M $AgNO_3$ solutions for the titrations. Stronger $AgNO_3$ solution was used for samples containing more than 10 mg dm^{-3} of cyanide whereas more dilute was used for samples containing 1-10 mg dm^{-3} of cyanide. The indicator solution was prepared by dissolving 0.03 g 5-(4-Dimethylaminobenzylidene)-rhodanine in 0.1 dm^3 acetone and stored in a dark bottle. The titrations were carried out with 0.005 dm^3 of cyanide solution to which

four drops of rhodamine indicator solution were added, after which the sample was titrated to a color change. Finally, the concentration of CN^- was calculated using Equation (3), where M is the molar mass (g mol^{-1}), V is volume (10^{-3} dm^3), and factor of reagent is 0.012255 for 0.00125 M $AgNO_3$ solution and 0.0012255 for 0.000125 M $AgNO_3$ solution.

$$Ag^+ + 2CN^- \rightarrow Ag(CN)_2^- \quad (1)$$

$$Ag^+ + Ag(CN)_2^- \rightarrow 2AgCN \quad (2)$$

$$CN^-(\text{mg dm}^{-3}) = \frac{M(NaCN)}{M(CN^-)} \cdot \frac{V(AgNO_3)}{V(\text{sample})} \cdot \text{factor of reagent} \cdot 10000 \quad (3)$$

In addition, ion chromatography by using a Metrohm 930 Compact IC Flex coupled to a conductivity detector was used to determine inorganic ions. The column Metrosep A Supp 7 located in an oven at 45 ºC with a mobile phase of 85:15 v/v 3.6 mM Na_2CO_3/acetone were used to analyze anions whereas cations were analyzed by using the column Metrosep C6 250 at 30 ºC with a mobile phase of 1.7 mM HNO_3 and 1.7 mM 2,6-pyridinedicarboxylic acid. The flow rates of mobile phases were 0.8 and 0.9 cm^3 min^{-1} to determine anions and cations, respectively. In both cases, 20 μL was the volume injection of each sample.

The total iron or aluminum concentration was measured off-line using an inductively coupled plasma Liberty Sequential Varian system according to the standard methods. The pH and conductivity were simultaneously measured using a Sension+ MM150 Portable Multi-Parameter Meter from HACH. The Total Organic Carbon (TOC) was determined using a Shimadzu TOC-VCPH analyzer and the theoretical TOC was calculated according to Equation 4 where $[CN^-]$ is referred to free cyanide that remains in solution, AW_C is the atomic weight of carbon (12 g mol^{-1}) and MW_{CN^-} is the molecular weight of

cyanide (26 g mol^{-1}). In addition, hypochlorite was analyzed by titration with 0.001 M As_2O_3 in 2 M NaOH [31, 32].

$$TOC_{th} = [CN^-] \cdot (AW_C/MW_{CN-}) \quad (4)$$

Finally, the sludge generated during both conventional and electrochemical coagulation was characterized by X-Ray Diffraction (XRD) analysis using a Philips PW-1710 instrument with Ni-filtered Cu kα radiation (λ: 1.5404 Å). Samples were scanned at a rate of 0.02º $step^{-1}$ within the range $10º \leq 2\theta \leq 90º$ and the diffractograms obtained were compared with the JCPDS-ICDD references.

3. Results and discussion

Figure 1 shows the percentage of cyanide removed during the chemical coagulation of 100 mg dm^{-3} of cyanide in mining wastewater. Every test was developed at pH 12 to ensure the stability of cyanide ion in aqueous solution avoiding the release of HCN. Thus, after the addition of the coagulant with the corresponding decrease in the pH, this parameter was rapidly modified up to 12.0. The coagulants tested were inorganic salts of iron ($FeCl_3$) and aluminum ($AlCl_3$) within the wide range 0.01 – 10 000 mg dm^{-3}. Ferric iron (Fe^{3+}) was selected as iron salt because the pH conditions used leads to a rapid oxidation of ferrous iron (Fe^{2+}) to ferric form in water [33].

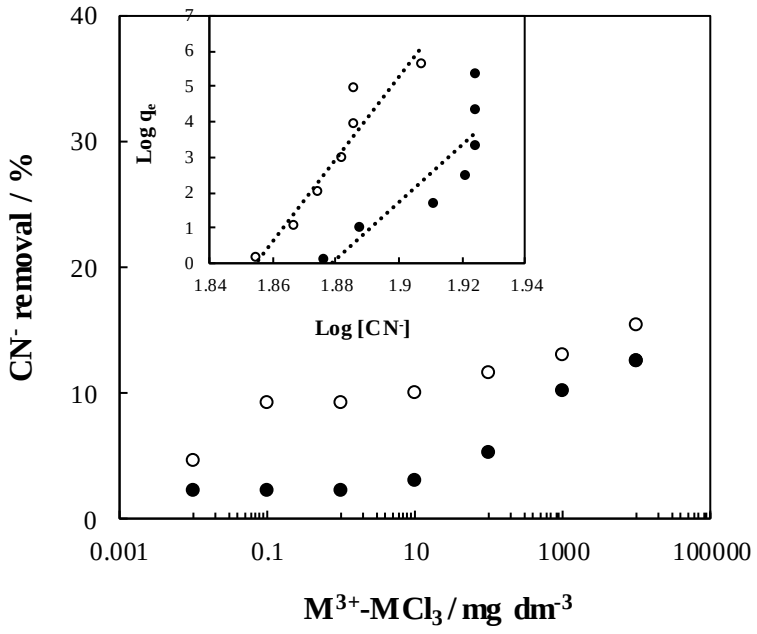

186

187 **Figure 1.** Cyanide removal percentage as a function of coagulant dosages during
188 chemical coagulation of synthetic mining wastewater intensified with 100 mg CN^- dm^{-3}
189 at pH of 12. Inorganic coagulants: Fe^{3+}-$FeCl_3$ (full symbols), Al^{3+}-$AlCl_3$ (empty
190 symbols). The inset shows data fitted to Freundlich isotherm.

191

192 As it can be seen, both reagents can help to remove cyanide, although the efficiency is
193 not very high and cyanide removal percentages during chemical coagulation are always
194 below 15%, even for the highest coagulant dosage of 10 000 mg dm^{-3}. This last value
195 generates a large amount of sludge in the final effluent and, for this reason, no higher
196 coagulant doses were used. In addition, the percentage of cyanide removed is higher with
197 the aluminum than with the iron coagulant dosages.

198 Initially, adsorption of the cyanide onto the growing hydroxide precipitates is the
199 expected primary mechanism to explain the removal of this pollutant. To confirm this
200 and, thus, to elucidate the possible mechanisms which control the removal of cyanide in

mining wastewater by using chemical coagulation processes, experimental data were fitted to Freundlich isotherm (Eq. 5) as shown in the inset of Figure 1. The Freundlich isotherm is an adsorption curve which relates the equilibrium concentration of a solute adsorbed onto the surface of a solid through chemisorption, physisorption or both (*q, mg CN^- adsorbed / g M-MCl_3*) with the concentration of the solute in the solution (*CN^-, mg dm^{-3}*). The models obtained for iron and aluminum adsorbents are shown in Equations 6 and 7, respectively. As observed, fitting of the experimental data to the model is not perfect and suggests that, in addition to adsorption, other processes must be contributing to the removal of cyanide. Thus, experimental data are observed to fit the Freundlich isotherm during aluminum chemical coagulation with a regression coefficient of 0.9047 whereas for chemical coagulation with iron, data fit the Freundlich isotherm with a lower regression coefficient of 0.7585. This fact supports the hypothesis made regarding that cyanide in mining wastewater is removed by adsorption onto aluminum or iron flocs formed during the chemical coagulation process. However, the extremely low values obtained for Freundlich's constant (K_F) indicates a low adsorption capacity from adsorbents added during chemical coagulation to remove cyanide from mining wastewater in comparison with other K_F values reported in literature [34-37] and the co-existence of other processes, most probably complexation processes.

$$q_e = K_F \cdot C_e^{1/n} \quad (5)$$

$$q = 4 \cdot 10^{-154} \cdot [CN^-]^{81.67} \quad (6)$$

$$q = 3 \cdot 10^{-216} \cdot [CN^-]^{116.25} \quad (7)$$

Coagulation and electrocoagulation technologies differ significantly in the way in which the coagulants are added to the wastewater and it is reported that this type of addition of

224 inorganic coagulants in solution may significantly affect the pollutant removal efficiency
225 of the coagulation process [38, 39]. The chemical coagulation process involves the
226 addition of inorganic salts, mainly iron or aluminum salts, as coagulants which alters the
227 physicochemical composition of the solution by increasing its conductivity. On the
228 contrary, the electrochemical coagulation process involves the in-situ generation of
229 coagulants through the electro-dissolution of a sacrificial anode, which is usually made
230 of iron or aluminum. At this point, Figure 2 shows the cyanide removal from mining
231 wastewater during electrochemical coagulation with iron (Figure 2a) and aluminum
232 (Figure 2b) electrodes. The electrochemical coagulation processes were developed within
233 the range of current densities 1 - 100 A m^{-2} and no passivation phenomena were observed
234 for all the tests carried out with both electrode materials.

235

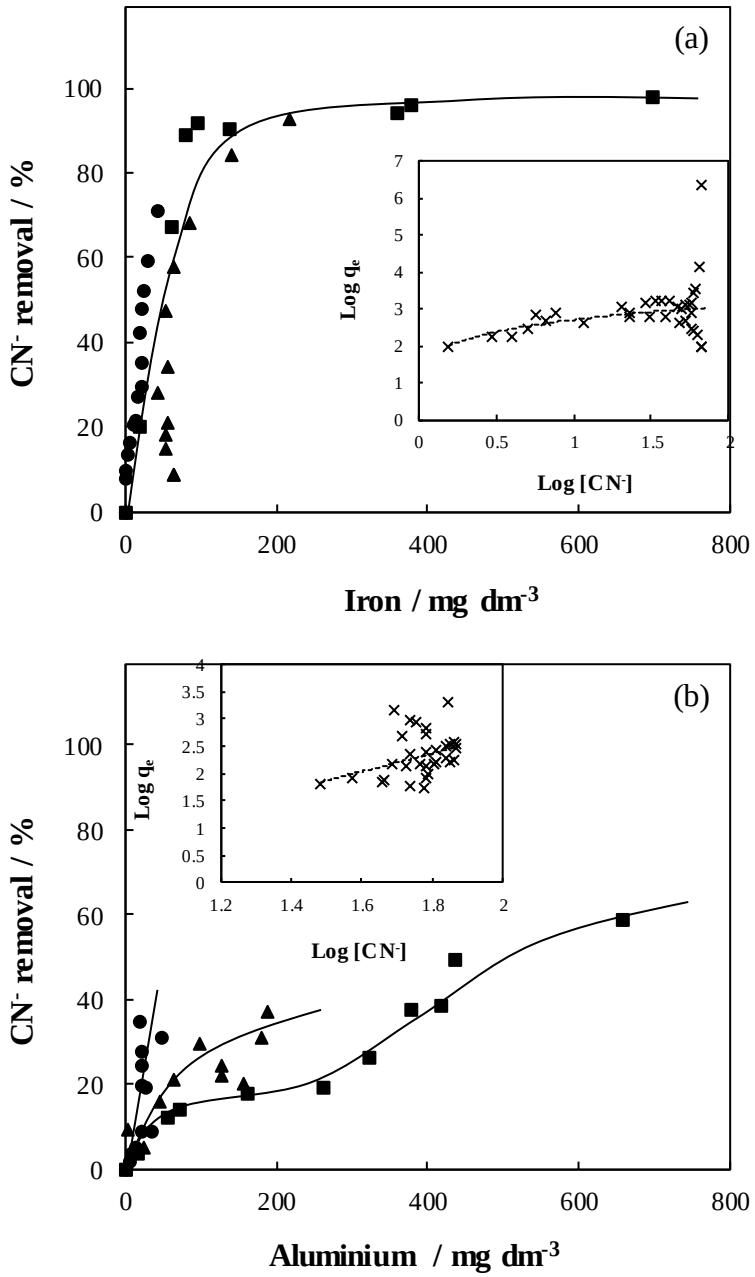

236

237 **Figure 2.** Cyanide removal percentage as a function of electrogenerated coagulant
238 concentration during electrochemical coagulation of synthetic mining wastewater
239 intensified with 100 mg CN^- dm^{-3} at initial pH of 12. Anode/Cathode: Fe/Fe (a), Al/Al
240 (b). Current density: (●) 1 A m^{-2}, (▲) 10 A m^{-2}, (■) 100 A m^{-2}. The insets show data fitted
241 to Freundlich isotherm.

242

243 Surprisingly, cyanide is completely removed from mining wastewater during
244 electrochemical coagulation at initial pH of 12 by using iron electrodes with almost
245 negligible influence of current density applied. However, less than 60% of cyanide
246 removal is attained for electrochemical coagulation with aluminum electrodes. In
247 addition, a significant influence of the current density on cyanide removal is clearly
248 observed with this electrode. Then, 50% of cyanide removal is reached for 50 mg dm^{-3} of
249 iron, regardless the current density applied whereas 40, 15 and 5% of cyanide removal is
250 achieved for the same dosage of aluminum during electrochemical coagulation at 1, 10
251 and 100 A m^{-2}, respectively. This fact means that iron is much more efficient than
252 aluminum for the removal of cyanide from mining wastewater when coagulants are dosed
253 by a sacrificial anode in the electrochemical coagulation processes, regardless of the
254 current density applied, opposite than the behavior observed during the chemical
255 coagulation processes. Furthermore, the higher current density applied, the lower is the
256 cyanide removal efficiency observed during aluminum electrochemical coagulation
257 processes.

258 For comparison purposes, and in order to know more about mechanisms, data obtained
259 during the iron and aluminum electrochemical coagulation processes were also fitted to a
260 Freundlich isotherm and plots are shown in the insets of Figure 2a and 2b, respectively.
261 In both cases, the theoretical Freundlich isotherm line does not fit well experimental data
262 as a high dispersion of experimental points can be observed with regression coefficients
263 of only 0.1269 for iron (Eq. 8) and 0.1158 for aluminum (Eq. 9). This fact confirms that
264 the main mechanism to remove cyanide from mining wastewater during electrochemical
265 coagulation is not adsorption onto iron or aluminum flocs as hypothesized during
266 chemical coagulation.

Here, it is noteworthy to point out that iron or aluminum speciation significantly depends on the dosage form, the pH of the solution and their concentration [38]. In this context, it is important to bear in mind that the pH was fixed at 12 for the chemical coagulation using the standard jar test experiments and corrected after the addition of the coagulants to reach again the same pH value (because the salts behave as Lewis acids) whereas for the electrochemical tests, pH was initially fixed at 12 and then, monitored along electrochemical coagulation processes without further changes, as in this case the net reagent dosed is iron or aluminum hydroxide, which does not behave as a Lewis acid. Thus, Figure 3 shows the evolution of coagulant-pH in the speciation maps for the removal of cyanide in mining wastewater during the iron (Figure 3a) and aluminum (Figure 3b) electrochemical coagulation processes within the range of current densities from 1 to 100 A m^{-2}, and during chemical coagulation tests with iron (Figure 3c) and aluminum (Figure 3d) salts. Initial pH was adjusted before start the experiments to a value of 12. In the case of chemical tests, this adjustment was carried out again after adding the coagulant since aluminium and iron salts decrease the solution pH.

$$q=121.43\cdot[CN^-]^{0.59} \quad (8)$$

$$q=0.32\cdot[CN^-]^{1.61} \quad (9)$$

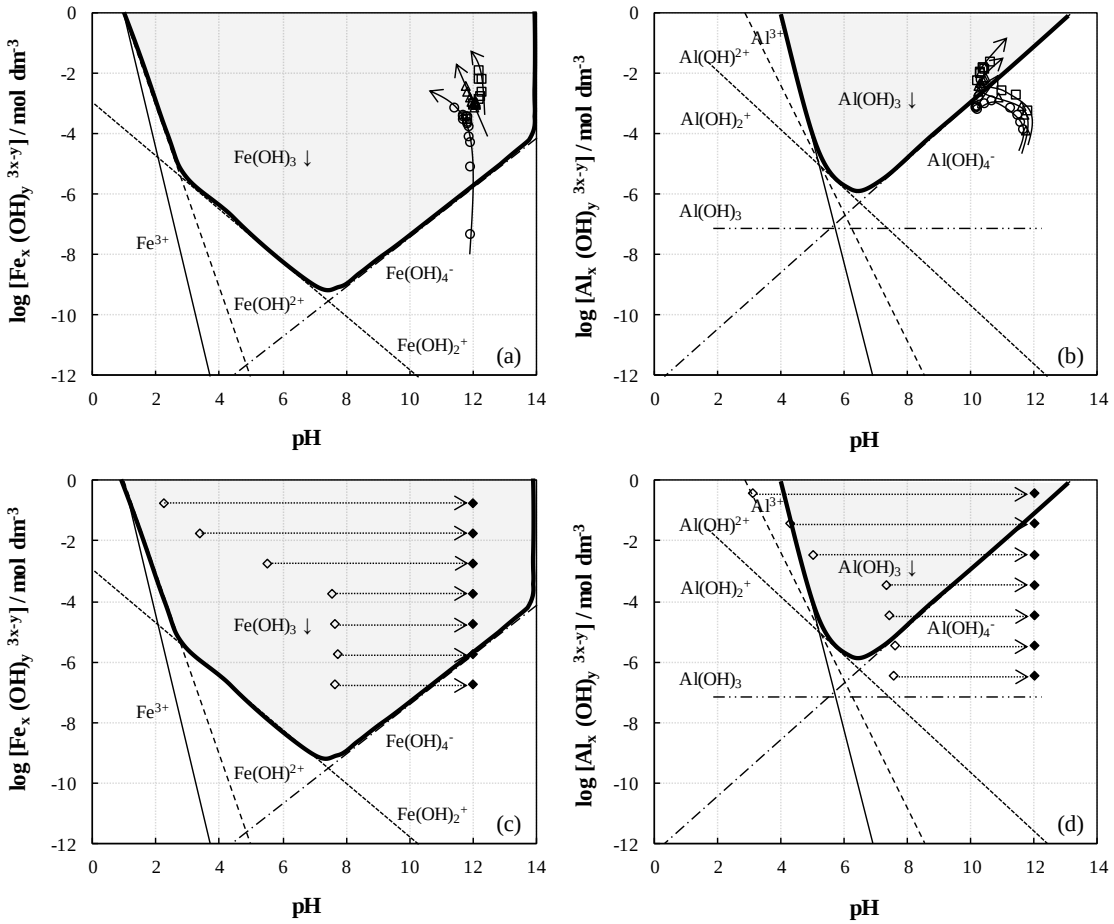

284

285 **Figure 3.** Coagulant-pH evolution during chemical and electrochemical coagulation of
286 synthetic mining wastewater intensified with 100 mg CN^- dm^{-3}. Electrochemical
287 coagulation: anode/cathode: Fe/Fe (a), Al/Al (b); current density: (○) 1 A m^{-2}, (Δ) 10 A
288 m^{-2}, (□) 100 A m^{-2}. Chemical coagulation: coagulant salts: $FeCl_3$ (c), $AlCl_3$ (d); pH
289 correction: initial pH (◊), corrected pH (♦). Arrows indicate the trends in pH during the
290 process

291

292 The pH is observed to be maintained in values close to 12 during iron electrochemical
293 coagulation regardless the current density applied and under these conditions, the
294 electrodissolved Fe^{+2} may be quickly oxidized and hydrolyzed to iron precipitate $Fe(OH)_3$
295 as the main ionic monomeric species in solution. Opposite, pH is observed to decrease

296 down to 10 throughout aluminum electrochemical coagulation and this decrease is faster
297 at lower current density values. Here, two different phases can be distinguished depending
298 on pH evolution. Firstly, the soluble ionic monomeric species $Al(OH)_4^-$ and $Al(OH)_3$ are
299 the main aluminum species in solution when pH decreases from 12 to 10 and secondly,
300 the aluminum precipitate $Al(OH)_3$ is the dominant aluminum species when pH is
301 maintained constant in a value of 10. Then, different pH behavior is observed depending
302 on coagulation process as pH was maintained in a constant value of 12 during chemical
303 coagulation at standard jar test experiments and, as a consequence, different iron or
304 aluminum species are present in solution depending on coagulation process. Regarding
305 the chemical coagulation tests, it can be seen how the initial addition of the coagulant
306 acidifies the mining wastewater from the initial value of 12 to a value which decreases
307 with the increasing coagulant dose and how during the tests, this acidification is
308 compensated with the addition of sodium hydroxide to reach pH 12 again, leading to a
309 very different expected speciation, which is much less efficient than that obtained by the
310 electrochemical process naturally. In addition, because of the expected high solubility of
311 aluminum hydroxide at pH 12, the presence of other precipitates should be expected,
312 which protects the insoluble product formed during the initial addition of the coagulant.

313 At this point, it is worth to take in mind that the bonding properties of cyanide ion make
314 it a very strong-field ligand for several transition metals [40]. Among others, cyanide ion
315 is capable of forming hexacyanides with titanium, vanadium, chrome, manganese, iron
316 or cobalt, tetracyanides with nickel, palladium or platinum and dicyanides with copper,
317 silver or gold. In this way, Figure 4 shows the TOC removal percentage as a function of
318 iron (Figure 4a) and aluminum (Figure 4b) electrogenerated concentrations for the
319 electrochemical coagulation treatment of synthetic mining wastewater intensified with
320 100 mg dm^{-3} of free cyanide, in order to study the possible formation of soluble cyano

metal complexes. TOC present in synthetic mining wastewater comes from the carbon in cyanide ion. In addition, the theoretical TOC removal calculated from Eq. 4 has also been plotted here.

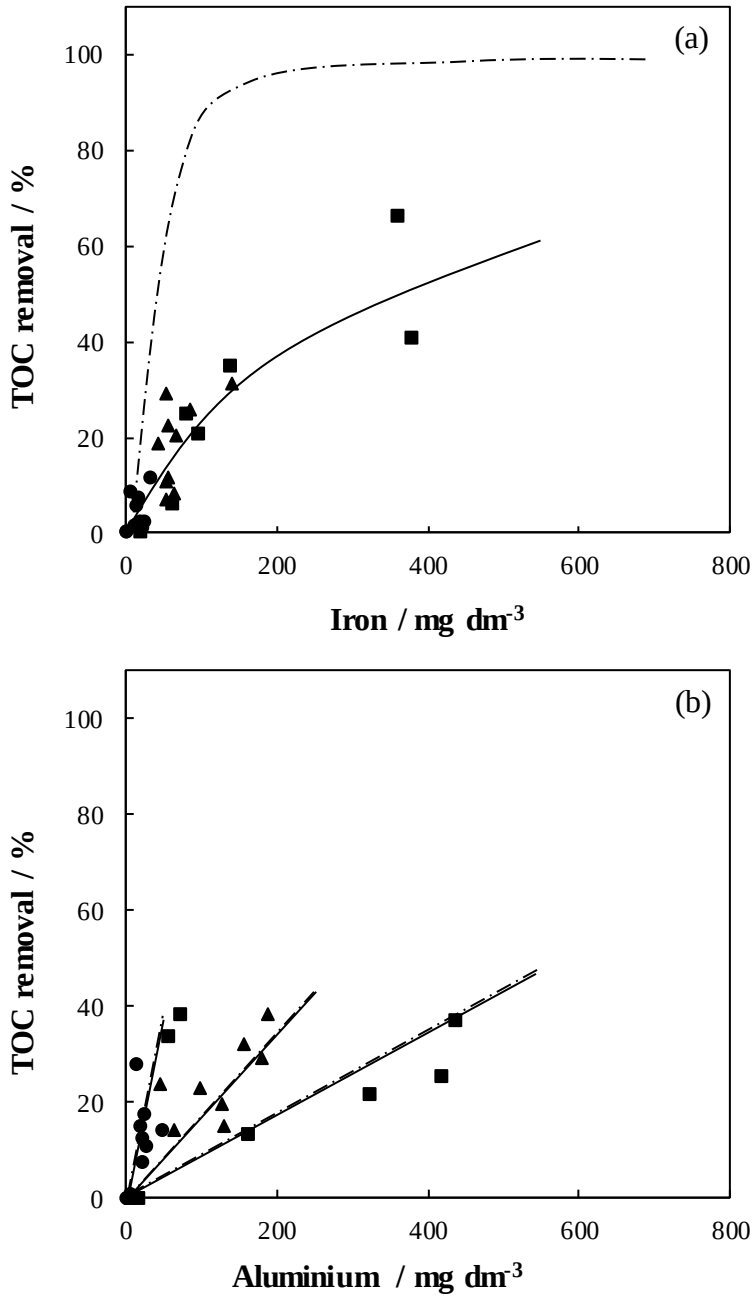

Figure 4. TOC removal percentage as a function of electrogenerated coagulant concentration during electrochemical coagulation of synthetic mining wastewater intensified with 100 mg CN^- dm^{-3}. Anode/Cathode: Fe/Fe (a), Al/Al (b). Current density:

(●) 1 A m^{-2}, (▲) 10 A m^{-2}, (■) 100 A m^{-2}. Dashdotted lines represent theoretical TOC removal according to experimental data.

Regarding the evolution of TOC removal percentage during the iron electrochemical coagulation, the result obtained is much lower than the expected value and no influence of the current density is observed. At the end of each experiment, the experimental TOC removal percentage is expected to be up to 100% *vs.* less than 60% of TOC removal percentage monitored. This fact suggests that free cyanide is not totally removed from solution and it could still remain as soluble cyano iron complexes in wastewater. According to literature, the complexation reactions between iron (II) and free cyanide ions may be described by Eqs. (10-12) [41]. Iron (II) is firstly electrodissolved from an iron electrode during electrochemical coagulation process and then, iron (II) reacts with free cyanide to form soluble ferrocyanide complex ($Fe(CN)_6^{4-}$) as shown in Equation (10). When the amount of ferrous ions increases throughout experimental time, $Fe(CN)_6^{4-}$ may be immobilized as an insoluble ferrocyanide ($Fe_2^{II}Fe^{II}(CN)_6$) which can be quickly oxidized to form insoluble ferric ferrocyanide ($Fe_4^{III}[Fe^{II}(CN)_6]_3$). However, the presence of soluble $Fe(CN)_6^{4-}$ in solution is much less toxic than free cyanide and its formation is essentially nontoxic except under UV-irradiating condition [42].

$$Fe^{+2} + 6CN^- \rightarrow Fe(CN)_6^{4-} \quad (10)$$

$$Fe^{+2} + Fe(CN)_6^{4-} \rightarrow Fe_2^{II}Fe^{II}(CN)_6\,(\downarrow) \quad (11)$$

$$Fe_2^{II}Fe^{II}(CN)_6 \rightarrow Fe_4^{III}[Fe^{II}(CN)_6]_3\,(\downarrow) + 2Fe^{+2} + 4e^- \quad (12)$$

On the other hand, TOC removal percentage overlaps with theoretical TOC removal percentage during aluminum electrochemical coagulation processes which means an

almost null formation of any soluble cyano aluminum complexes. In addition, a significant influence of the current density is observed. The lower current density applied the higher TOC removal efficiency is attained. Nevertheless, the maximum TOC removal percentage reached is below 40%, regardless of the current density applied.

In this context, the mechanisms proposed for free cyanide removal from synthetic mining wastewater by means of both iron and aluminum electrochemical coagulation processes is schematically drawn in Figure 5. It is important to consider that the release of Fe^{+2} from an iron plate anode leads to the formation of soluble and/or insoluble metal-cyanide complexes during the iron electrochemical coagulation process. The presence of soluble metal-cyanide complexes allows the toxicity of solution to drastically decrease in comparison with the initial toxicity of free cyanide. On the other hand, free cyanide is removed by charge neutralization with soluble $Al(OH)_3$ during the aluminum electrochemical coagulation process. Finally, free cyanide may also be removed thanks to its adsorption on a superficially charged metal precipitate and its enmeshment into a sweep metal floc in both electrochemical coagulation processes.

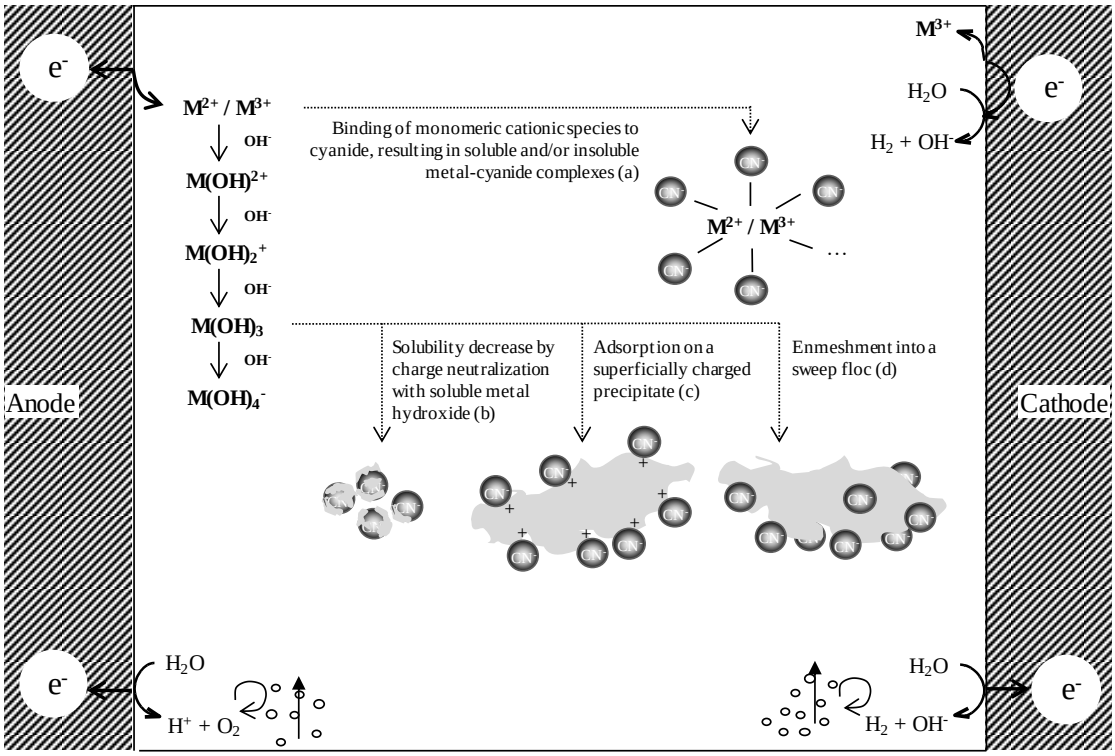

366

367 **Figure 5.** Mechanisms proposed for cyanide removal from synthetic mining wastewater
368 during electrochemical coagulation. Anode/Cathode: Fe/Fe (a, c, d), Al/Al (b, c, d).

369

370 The mechanism proposed for cyanide removal may be supported by the characterization
371 of the sludge generated after the coagulation treatment (shown in Figure 6). The XRD
372 analysis of the resultant sludge from chemical coagulation treatments with $FeCl_3$ (Figure
373 6a) shows the main diffraction goethite ($Fe^{3+}O(OH)$) peaks (110), (130), (021), (111),
374 (121), (140), (221), (160), (250) and (061) at 2θ = 21.1º, 33.3º, 34.7º, 36.6°, 39.9º, 41.2º,
375 53.2º, 59.1º, 61.4º and 64.1º, respectively. However, the XRD analysis for the sludge
376 generated during electrochemical coagulation with iron electrodes (Figure 6c) confirms
377 not only the presence of the magnetite ($Fe^{2+}(Fe^{3+})_2O_4$) peaks (220), (311), (400) (511)
378 and (440) at 2θ = 30.1º, 35.4°, 43.0º, 57.1º and 62.7º, respectively, but also the appearance
379 of the ferric ferrocyanide ($Fe_4^{III}[Fe^{II}(CN)_6]_3$) peak (321) at 2θ = 28°. This fact could justify

the formation of the cyano iron (II) complexes (Eqs. 10-12) in solution as a significant mechanism to remove free cyanide during electrochemical coagulation with iron electrodes, in comparison to its removal by adsorption onto iron (III) oxide-hydroxide. On the other hand, Figure 6b shows a mixture of bayerite (α-$Al(OH)_3$) peaks (001), (101), (111) and (112) at 2θ = 18.7º, 27.9º, 40.6° and 53.2º, respectively, and gibbsite (γ-$Al(OH)_3$) peaks (110) and (023) at 2θ = 20.3° and 45.4º for chemical coagulation with $AlCl_3$. However, only the bayerite (α-$Al(OH)_3$) peaks (001), (101), (111) and (112) at 2θ = 18.7º, 27.9º, 40.6° and 53.2º, respectively, are observed for the electrochemical coagulation with aluminum electrodes in Figure 6d. Here, the difference between gibbsite and its other polymorphs, such as bayerite, consists of a slightly different arrangement of hydroxyl groups which make bayerite more efficient for the removal of free cyanide.

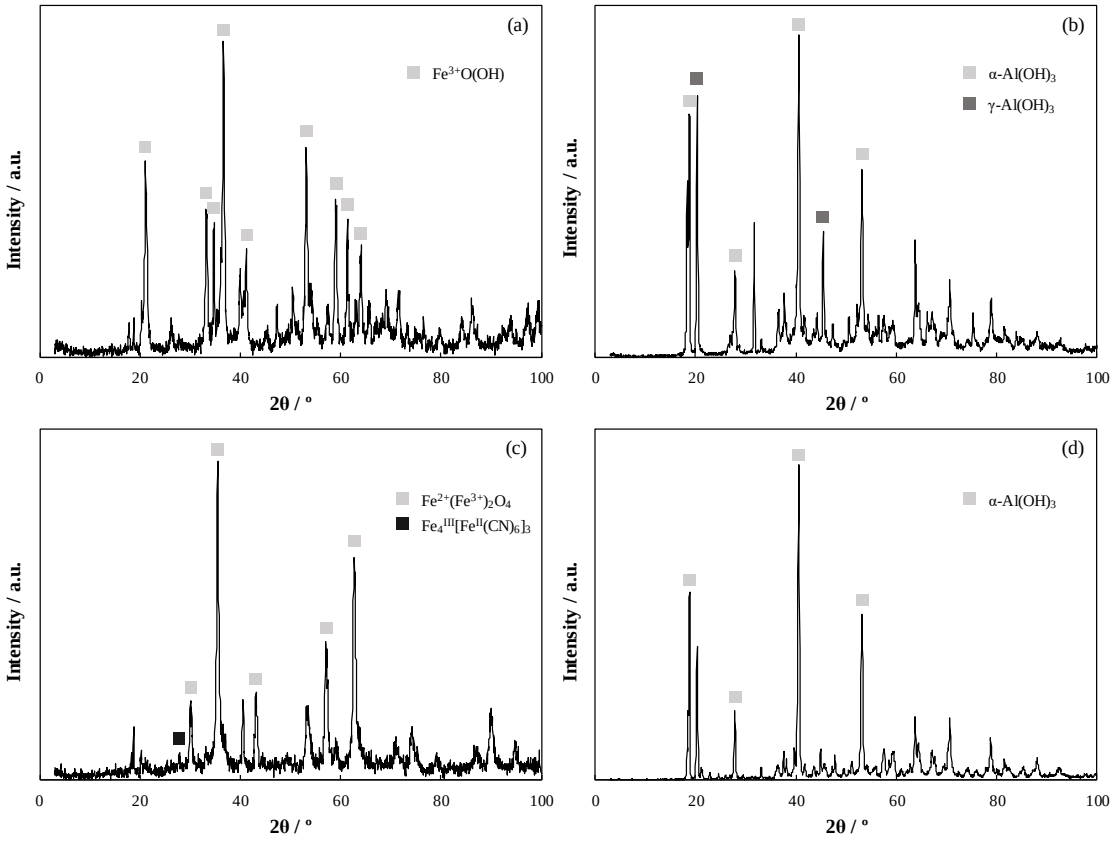

393 **Figure 6.** XRD analysis of the sludge generated after the coagulation treatment of
394 synthetic mining wastewater intensified with 100 mg CN^- dm^{-3}: (a) chemical coagulation
395 with 1000 mg $FeCl_3$ dm^{-3}, (b) chemical coagulation with 1000 mg $AlCl_3$ dm^{-3}, (c)
396 electrochemical coagulation with Fe electrodes at 100 A m^{-2}, (d) electrochemical
397 coagulation with Al electrodes at 100 A m^{-2}.

398

399 In order to go more in-depth, the chemical and/or electrochemical reactivity has also been
400 studied for the different species involved in mining wastewater (3000 mg SO_4^{2-} dm^{-3}, 300
401 mg Cl^- dm^{-3}, 60 mg NO_3^- dm^{-3}, 30 mg NH_4^+ dm^{-3} and 100 mg CN^- dm^{-3}) in order to
402 determine the possible formation of hazardous species.

403 Regardless of the possible oxidation of cyanide to form cyanate (CNO^-), CNO^- has been
404 not detected by ionic chromatography along with any electrochemical coagulation tests.
405 Anyway, CNO^- is well known to quickly decompose as shown in Equation 13. Regarding
406 the formation of other hazardous inorganic species, it is especially important to focus on
407 the chlorine species because chloride may be electrooxidized to chlorine (Eq. 14) and
408 thus, it disproportionates to hypochlorite (Eqs. 15-16) or is further oxidized to other
409 chlorine compounds in higher oxidation state, such as chlorate or perchlorate (Eqs. 17-
410 19) [43]. These high oxidation state chlorine compounds are reported to be hazardous to
411 human health [44, 45]. For this reason, the evolution of chlorine species has been
412 monitored along with iron and aluminum electrochemical coagulation processes as shown
413 in Figure 7a and 7b, respectively.

414 $$CNO^- + 2H_2O \rightarrow CO_3^{2-} + NH_4^+ \quad (13)$$

415 $$2\ Cl^- \rightarrow Cl_2 + 2\ e^- \quad (14)$$

$$Cl_2 + H_2O \rightarrow HClO + Cl^- + H^+ \quad (15)$$

$$HClO \leftrightarrows H^+ + ClO^- \quad (16)$$

$$ClO^- + H_2O \rightarrow ClO_2^- + 2\,H^+ \quad (17)$$

$$ClO_2^- + H_2O \rightarrow ClO_3^- + 2\,H^+ \quad (18)$$

$$ClO_3^- + H_2O \rightarrow ClO_4^- + 2\,H^+ \quad (19)$$

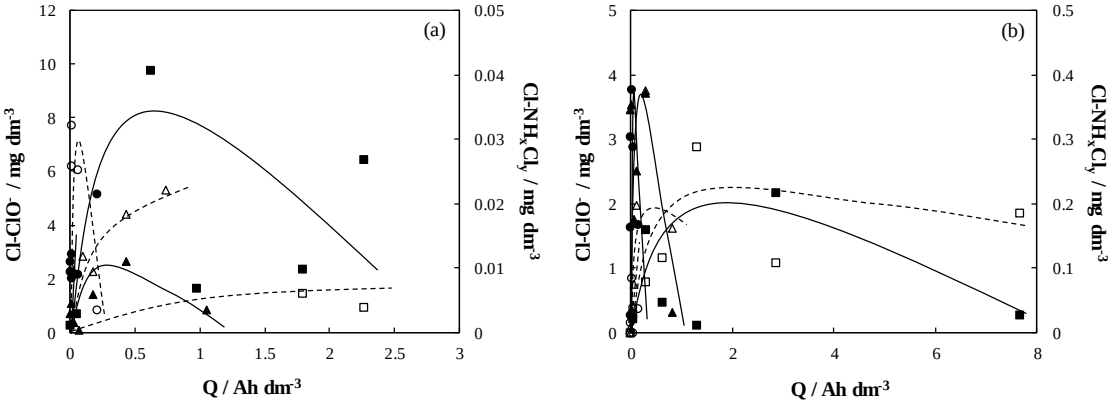

Figure 7. Hypochlorite (full symbols) and chloramines (empty symbols) concentrations as a function of applied electric charge during electrochemical coagulation of synthetic mining wastewater intensified with 100 mg CN^- dm^{-3}. Anode/Cathode: Fe/Fe (a), Al/Al (b). Current density: (●) 1 A m^{-2}, (▲) 10 A m^{-2}, (■) 100 A m^{-2}.

Chloride is observed to be transformed into hypochlorite which behaves as a reaction intermediate. The higher the current density applied, the higher is the hypochlorite concentration regardless of iron or aluminum electrochemical coagulation processes. The maximum hypochlorite concentration detected in solution is up to 10 mg $Cl\text{-}ClO^-$ dm^{-3}

for iron electrochemical coagulation although it is below 4 mg Cl-ClO^- dm^{-3} for aluminum electrochemical coagulation. Opposite to it could be expected, hypochlorite does not undergo further oxidation to hazardous chlorine species such as chlorate or perchlorate because these chlorine species have been not detected in solution along with any electrochemical coagulation tests. On the contrary, hypochlorite is well known to chemically react with ammonium ions and then, it results in the production of inorganic chloramines as shown in Equations 20-22 [46, 47].

$$NH_4^+ + ClO^- \rightarrow NH_2Cl + H_2O \quad (20)$$

$$NH_2Cl + ClO^- \rightarrow NHCl_2 + H_2O \quad (21)$$

$$NHCl_2 + ClO^- \rightarrow NCl_3 + H_2O \quad (22)$$

As can be observed, the presence of chloramines in solution is influenced by current density applied. The concentration of chloramines ranges from 0.01 to 0.03 mg dm^{-3} during iron electrochemical coagulation and this concentration increases up to 10 times for aluminum electrochemical coagulation. This fact may be explained bearing in mind the chemical reduction of nitrate to ammonium ions by aluminum as shown in Equations 23 and 24 [48, 49]. This confirms the higher concentration of chloramines during aluminum electrochemical coagulation, in comparison with their concentration during iron electrochemical coagulation because of the increase of ammonium ions in solution with aluminum electrodes.

$$3NO_3^- + 2Al + 3H_2O \rightarrow 3NO_2^- + 2Al(OH)_3 \quad (23)$$

$$NO_2^- + 2Al + 5H_2O \rightarrow NH_3 + 2Al(OH)_3 + OH^- \quad (24)$$

Finally, Figure 8 shows the energy consumption as a function of the current density (1-100 A m^{-2}) for the removal not only of the target organic pollutant cyanide but for the inorganic pollutants presented in mining wastewater such as nitrate, ammonium ions and sulfate during both iron and aluminum electrochemical coagulation processes.

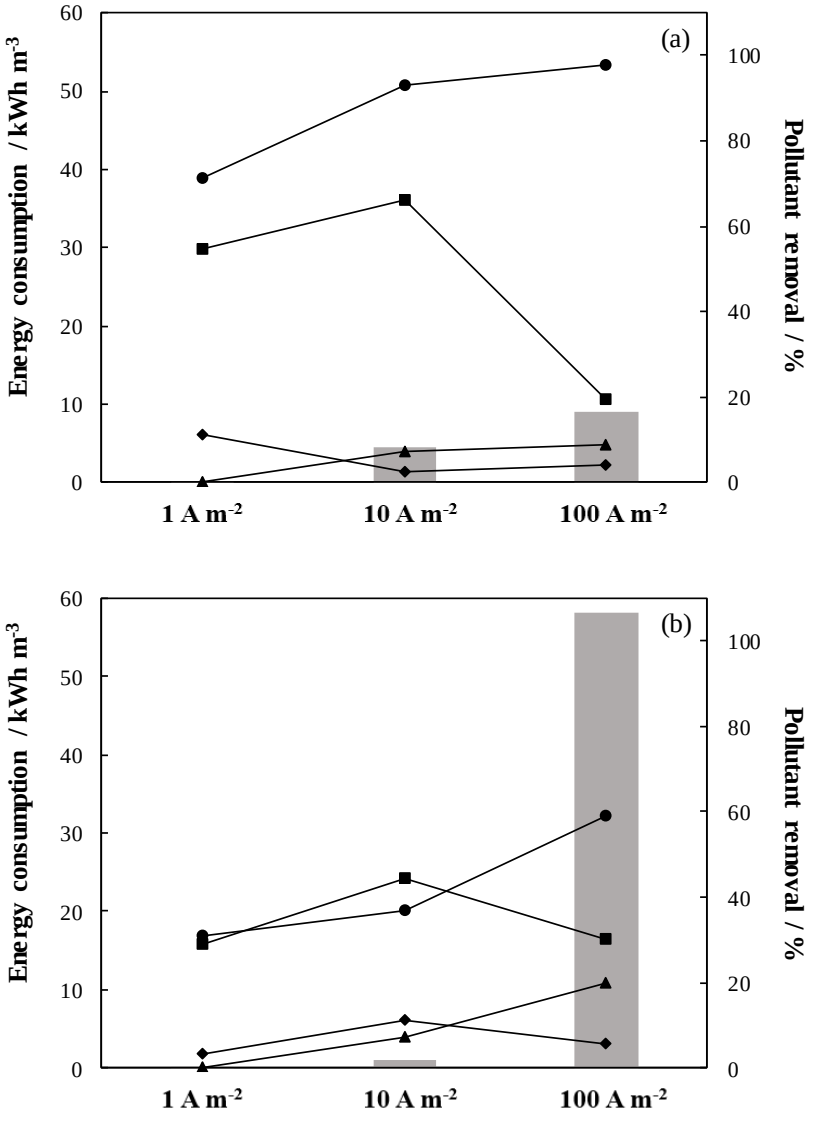

Figure 8. Influence of current density on energy consumption (bars) for pollutants removal (points) during electrochemical coagulation of synthetic mining wastewater

intensified with 100 mg CN^- dm^{-3}. Anode/Cathode: Fe/Fe (a), Al/Al (b). Pollutant species: (●) CN^-, (▲) NO_3^-, (■) NH_4^+, (♦) SO_4^{2-}.

As expected, the energy consumption increases with current density, regardless of the electrode material tested in electrochemical coagulation. However, at the highest current density 10 kWh m^{-3} are required to remove 100% of cyanide from mining wastewater during iron electrochemical coagulation, whereas 60 kWh m^{-3} are only able to attain 60% of cyanide removal for aluminum electrochemical coagulation. The higher energy consumption with aluminum electrodes may be explained by the higher cell potential needed to electrochemically release the coagulant due to its passivation layer. Likewise, inorganic species from mining wastewater are also removed during both electrochemical coagulation processes although in a much lower range than the target pollutant. Thus, at 10 A m^{-2} the removal percentage of nitrates is 7.5 and 7.2 %, for ammonium ions is 66.2 and 44.4 % and for sulfates is 2.4 and 11.0 % during iron and aluminum electrochemical coagulation, respectively. The results obtained for the removal of nitrates are in agreement with previous works reported in the literature [49], where the same amount of nitrate removal was obtained for the same reagent dose using both iron and aluminum anodes. Nitrate removal can be explained by adsorption onto growing metal hydroxide precipitates. Moreover, the lower removal of ammonium ions with aluminum electrodes than with iron ones may be explained due to their production by the chemical reaction between nitrates and aluminum which increases their concentration in solution [48]. Finally, the removal percentages for sulfates are very low because sulfate may be efficiently removed from mining wastewater by coagulation although at acidic pHs [12].

4. Conclusions

From this work, the following conclusions can be drawn:

- Chemical coagulation at pH of 12 leads to a maximum cyanide removal percentage from mining wastewater of 15%. Although it is not the unique, adsorption onto metal flocs is the primary mechanism that explains results. Experimental data are fitted to Freundlich isotherm with correlation coefficients of 0.7585 for Fe-$FeCl_3$ and 0.9047 for Al-$AlCl_3$.
- Electrochemical coagulation with iron electrodes leads to the complete cyanide removal from mining wastewater at initial pH of 12, regardless of the current density value applied. However, a maximum cyanide removal of 60% is attained during electrochemical coagulation with aluminum electrodes at the highest current density value tested (100 A m^{-2}). The cyanide removal does not fit well to Freundlich isotherm with low correlation coefficients (r^2_{Fe}=0.1269, r^2_{Al}=0.1158) which means that the main coagulation mechanism is not an adsorption process in this case.
- Electrochemical coagulation with iron electrodes allows the formation of soluble and/or insoluble iron-cyanide complexes due to the release of Fe^{+2} from the iron plate anode. In electrochemical coagulation with aluminum electrodes, cyanide decreases its solubility by charge neutralization with aluminum soluble metal hydroxide. Likewise, cyanide may also be removed by adsorption on a superficially charged metal precipitate and enmeshment into a sweep metal floc in both cases.
- Chemical and/or electrochemical reactivity of cyanide and inorganic species from mining wastewater is also studied. A null detection of cyanate or inorganic chlorine hazardous species such as chlorate or perchlorate is found through

electrochemical coagulation tests. However, chloride oxidizes to hypochlorite and hypochlorite concentrations up to 10 and 4 mg dm^{-3} are measured for iron and aluminum electrochemical coagulation, respectively. Likewise, hypochlorite behaves as intermediate because it chemically reacts with ammonium ions (contained in mining wastewater or produced by chemical reduction of nitrate by aluminum) to form chloramines in a concentration up to 0.3 mg dm^{-3} during aluminum electrochemical coagulation.

- The energy consumption required to remove 100% of cyanide from mining wastewater is 10 kWh m^{-3} during iron electrochemical coagulation at the highest current density value, whereas 60 kWh m^{-3} only attains 60% of cyanide removal along with aluminum electrochemical coagulation. In addition, other inorganic species from mining wastewater may be simultaneously removed during electrochemical coagulation processes.

Acknowledgments

Paula Vehmaanperä is gratefully acknowledged for the development of the analytical method to measure cyanide concentration from aqueous solutions. Financial support from the Spanish Ministry of Economy, Industry and Competitiveness and European Union through project CTM2016-76197-R (AEI/FEDER, UE) and from EIT Raw Materials (European Institute of Innovation and Technology) through project EWT-CYNCOR is gratefully acknowledged. Dr. Salvador Cotillas (SBPLY/16/180501/000404) and Miguel Herraiz-Carboné (SBPLY/18/180501/000009) wish to express their gratitude to the financial support of their grants from Junta de Comunidades de Castilla-La Mancha (JCCM).

References

[1] X. Yu, R. Xu, C. Wei, H. Wu, Removal of cyanide compounds from coking wastewater by ferrous sulfate: Improvement of biodegradability, Journal of Hazardous Materials, 302 (2016) 468-474.

[2] E. Iakovleva, M. Sillanpää, C. Mangwandi, A.B. Albadarin, P. Maydannik, S. Khan, V. Srivastava, K. Kamwilaisak, S. Wang, Application of Al2O3 modified sulfate tailings (CaFe-Cake and SuFe) for efficient removal of cyanide ions from mine process water, Minerals Engineering, 118 (2018) 24-32.

[3] N. Kuyucak, A. Akcil, Cyanide and removal options from effluents in gold mining and metallurgical processes, Minerals Engineering, 50-51 (2013) 13-29.

[4] J.R. Parga, S.S. Shukla, F.R. Carrillo-Pedroza, Destruction of cyanide waste solutions using chlorine dioxide, ozone and titania sol, Waste Management, 23 (2003) 183-191.

[5] T.I. Mudder, M.M. Botz, Cyanide and society: a critical review, European Journal of Mineral Processing & Environmental Protection, 4 (2004) 62-74.

[6] J. Cui, X. Wang, Y. Yuan, X. Guo, X. Gu, L. Jian, Combined ozone oxidation and biological aerated filter processes for treatment of cyanide containing electroplating wastewater, Chemical Engineering Journal, 241 (2014) 184-189.

[7] X. Zhao, J. Zhang, J. Qu, Photoelectrocatalytic Oxidation of Cu-cyanides and Cu-EDTA at TiO<inf>2</inf> nanotube electrode, Electrochimica Acta, 180 (2015) 129-137.

[8] R.R. Dash, C. Balomajumder, A. Kumar, Removal of cyanide from water and wastewater using granular activated carbon, Chemical Engineering Journal, 146 (2009) 408-413.

[9] L. Seung-Mok, T. Diwakar, Application of ferrate(VI) in the treatment of industrial wastes containing metal-complexed cyanides: A green treatment, Journal of Environmental Sciences, 21 (2009) 1347-1352.

[10] Y. Xu, J. Zhang, Y. Liang, J. Zhou, J. Zhao, X. Ruan, Z.P. Xu, G. Qian, Synchronous cyanide purification with metals removal in the co-treatment of Zn-CN and Ni electroplating wastewaters via the Ni2+-assisted precipitation of LDH, Separation and Purification Technology, 145 (2015) 92-97.

[11] C.A. Martínez-Huitle, M.A. Rodrigo, I. Sirés, O. Scialdone, Single and Coupled Electrochemical Processes and Reactors for the Abatement of Organic Water Pollutants: A Critical Review, Chemical Reviews, 115 (2015) 13362-13407.

[12] M.A. Mamelkina, S. Cotillas, E. Lacasa, C. Sáez, R. Tuunila, M. Sillanpää, A. Häkkinen, M.A. Rodrigo, Removal of sulfate from mining waters by electrocoagulation, Separation and Purification Technology, 182 (2017) 87-93.

[13] S. Cotillas, E. Lacasa, M. Herraiz, C. Sáez, P. Cañizares, M.A. Rodrigo, The Role of the Anode Material in Selective Penicillin G Oxidation in Urine, ChemElectroChem, 6 (2019) 1376-1384.

[14] Z. Ye, E. Brillas, F. Centellas, P.L. Cabot, I. Sirés, Electrochemical treatment of butylated hydroxyanisole: Electrocoagulation versus advanced oxidation, Separation and Purification Technology, 208 (2019) 19-26.

[15] S. Cotillas, M.J.M. de Vidales, J. Llanos, C. Sáez, P. Cañizares, M.A. Rodrigo, Electrolytic and electro-irradiated processes with diamond anodes for the oxidation of persistent pollutants and disinfection of urban treated wastewater, Journal of Hazardous Materials, 319 (2016) 93-101.

581 [16] S. Cotillas, J. Llanos, P. Cañizares, S. Mateo, M.A. Rodrigo, Optimization of an
582 integrated electrodisinfection/electrocoagulation process with Al bipolar electrodes for
583 urban wastewater reclamation, Water Research, 47 (2013) 1741-1750.
584 [17] F.L. Souza, M.R.V. Lanza, J. Llanos, C. Sáez, M.A. Rodrigo, P. Cañizares, A wind-
585 powered BDD electrochemical oxidation process for the removal of herbicides, Journal
586 of Environmental Management, 158 (2015) 36-39.
587 [18] M. Millán, M.A. Rodrigo, C.M. Fernández-Marchante, S. Díaz-Abad, M.C. Peláez,
588 P. Cañizares, J. Lobato, Towards the sustainable powering of the electrocoagulation of
589 wastewater through the use of solar-vanadium redox flow battery: A first approach,
590 Electrochimica Acta, 270 (2018) 14-21.
591 [19] F.L. Souza, C. Saéz, J. Llanos, M.R.V. Lanza, P. Cañizares, M.A. Rodrigo, Solar-
592 powered electrokinetic remediation for the treatment of soil polluted with the herbicide
593 2,4-D, Electrochimica Acta, 190 (2016) 371-377.
594 [20] S.O. Ganiyu, L.R.D. Brito, E.C.T. de Araújo Costa, E.V. dos Santos, C.A. Martínez-
595 Huitle, Solar photovoltaic-battery system as a green energy for driven electrochemical
596 wastewater treatment technologies: Application to elimination of Brilliant Blue FCF dye
597 solution, Journal of Environmental Chemical Engineering, 7 (2019) 102924.
598 [21] P. Cañizares, M. Díaz, J.A. Domíguez, J. Lobato, M.A. Rodrigo, Electrochemical
599 treatment of diluted cyanide aqueous wastes, Journal of Chemical Technology and
600 Biotechnology, 80 (2005) 565-573.
601 [22] M.R.V. Lanza, R. Bertazzoli, Selection of a commercial anode oxide coating for
602 electro-oxidation of cyanide, Journal of the Brazilian Chemical Society, 13 (2002) 345-
603 351.
604 [23] S.C. Cheng, M. Gattrell, T. Guena, B. MacDougall, The electrochemical oxidation
605 of alkaline copper cyanide solutions, Electrochimica Acta, 47 (2002) 3245-3256.

606 [24] C. Antonio Pineda Arellano, S.S. Martínez, Indirect electrochemical oxidation of
607 cyanide by hydrogen peroxide generated at a carbon cathode, International Journal of
608 Hydrogen Energy, 32 (2007) 3163-3169.
609 [25] S. Pulkka, M. Martikainen, A. Bhatnagar, M. Sillanpää, Electrochemical methods
610 for the removal of anionic contaminants from water – A review, Separation and
611 Purification Technology, 132 (2014) 252-271.
612 [26] G. Moussavi, F. Majidi, M. Farzadkia, The influence of operational parameters on
613 elimination of cyanide from wastewater using the electrocoagulation process,
614 Desalination, 280 (2011) 127-133.
615 [27] G. Hassani, S. Nasseri, H. Gharibi, Removal of cyanide by electrocoagulation
616 process, Analytical and Bioanalytical Electrochemistry, 3 (2011) 625-634.
617 [28] P. Cañizares, F. Martínez, J. Lobato, M.A. Rodrigo, Electrochemically assisted
618 coagulation of wastes polluted with eriochrome black T, Industrial and Engineering
619 Chemistry Research, 45 (2006) 3474-3480.
620 [29] E. Lacasa, P. Cañizares, C. Sáez, F.J. Fernández, M.A. Rodrigo, Electrochemical
621 phosphates removal using iron and aluminium electrodes, Chemical Engineering Journal,
622 172 (2011) 137-143.
623 [30] J.A. Ryan, G.W. Culshaw, The use of p-dimethylaminobenzylidene rhodanine as an
624 indicator for the volumetric determination of cyanides, Analyst, 69 (1944) 370-371.
625 [31] A.v. Wilpert, Über die Analyse von Hypochlorit und Chlorit in einer Lösung, Z.
626 Anal. Chem., 155 (1957) 378-378.
627 [32] H. Freytag, Zur Bestimmung von Hypochlorit, Chlorid und Chlorat in Chlorkalk, Z.
628 Anal. Chem., 171 (1959) 458-458.

[33] P. Cañizares, C. Jiménez, F. Martínez, M.A. Rodrigo, C. Sáez, The pH as a key parameter in the choice between coagulation and electrocoagulation for the treatment of wastewaters, Journal of Hazardous Materials, 163 (2009) 158-164.

[34] M. Tyagi, A. Rana, S. Kumari, S. Jagadevan, Adsorptive removal of cyanide from coke oven wastewater onto zero-valent iron: Optimization through response surface methodology, isotherm and kinetic studies, Journal of Cleaner Production, 178 (2018) 398-407.

[35] A. Samiee Beyragh, M. Varsei, M. Meshkini, A. Khodadadi Darban, E. Gholami, Kinetics and Adsorption Isotherms Study of Cyanide Removal from Gold Processing Wastewater Using Natural and Impregnated Zeolites, Iranian Journal of Chemistry and Chemical Engineering (IJCCE), 37 (2018) 139-149.

[36] N. Dwivedi, C. Balomajumder, P. Mondal, Comparative investigation on the removal of cyanide from aqueous solution using two different bioadsorbents, Water Resources and Industry, 15 (2016) 28-40.

[37] H.J. El-Aila, K.M. Elsousy, K.A. Hartany, Kinetics, equilibrium, and isotherm of the adsorption of cyanide by MDFSD, Arabian Journal of Chemistry, 9 (2016) S198-S203.

[38] P. Cañizares, F. Martínez, C. Jiménez, J. Lobato, M.A. Rodrigo, Comparison of the aluminum speciation in chemical and electrochemical dosing processes, Industrial and Engineering Chemistry Research, 45 (2006) 8749-8756.

[39] P. Cañizares, F. Martínez, C. Jiménez, J. Lobato, M.A. Rodrigo, Coagulation and electrocoagulation of wastes polluted with dyes, Environmental Science and Technology, 40 (2006) 6418-6424.

[40] C. Racaud, K. Groenen Serrano, A. Savall, Voltammetric determination of the critical micellar concentration of surfactants by using a boron doped diamond anode, Journal of Applied Electrochemistry, 40 (2010) 1845-1851.

654 [41] X. Yu, R. Xu, C. Wei, H. Wu, Removal of cyanide compounds from coking
655 wastewater by ferrous sulfate: Improvement of biodegradability, J Hazard Mater, 302
656 (2016) 468-474.
657 [42] P. Kjeldsen, Behaviour of cyanides in soil and groundwater: A review, Water, Air,
658 and Soil Pollution, 115 (1999) 279-307.
659 [43] A. Sánchez-Carretero, C. Sáez, P. Cañizares, M.A. Rodrigo, Electrochemical
660 production of perchlorates using conductive diamond electrolyses, Chemical Engineering
661 Journal, 166 (2011) 710-714.
662 [44] Y. Kurokawa, T. Imazawa, M. Matsushima, N. Takamura, Y. Hayashi, Lack of
663 Promoting Effect of Sodium Chlorate and Potassium Chlorate in Two-Stage Rat Renal
664 Carcinogenesis, Journal of the American College of Toxicology, 4 (1985) 331-337.
665 [45] J.R. Lubbers, S. Chauan, J.R. Bianchine, Controlled clinical evaluations of chlorine
666 dioxide, chlorite and chlorate in man, Environmental health perspectives, 46 (1982) 57-
667 62.
668 [46] E. Lacasa, J. Llanos, P. Cañizares, M.A. Rodrigo, Electrochemical denitrificacion
669 with chlorides using DSA and BDD anodes, Chemical Engineering Journal, 184 (2012)
670 66-71.
671 [47] S. Cotillas, J. Llanos, K. Castro-Ríos, G. Taborda-Ocampo, M.A. Rodrigo, P.
672 Cañizares, Synergistic integration of sonochemical and electrochemical disinfection with
673 DSA anodes, Chemosphere, 163 (2016) 562-568.
674 [48] A.P. Murphy, Chemical removal of nitrate from water, Nature, 350 (1991) 223-225.
675 [49] E. Lacasa, P. Cañizares, C. Sáez, F.J. Fernández, M.A. Rodrigo, Removal of nitrates
676 from groundwater by electrocoagulation, Chemical Engineering Journal, 171 (2011)
677 1012-1017.
678